Enhanced anxiety and stress-induced corticosterone release are associated with increased *Crh* expression in a mouse model of Rett syndrome

Bryan E. McGill*†, Sharyl F. Bundle‡, Murat B. Yaylaoglu§, James P. Carson§¶, Christina Thaller§, and Huda Y. Zoghbi*‡‖††‡‡**

*Department of Neuroscience, †Medical Scientist Training Program, ‡Department of Molecular and Human Genetics, §Verna and Marrs McLean Department of Biochemistry and Molecular Biology, ¶National Center for Macromolecular Imaging, ‖Department of Neurology, **Department of Pediatrics, and ††Howard Hughes Medical Institute, Baylor College of Medicine, Houston, TX 77030

Contributed by Huda Y. Zoghbi, October 2, 2006 (sent for review September 14, 2006)

Rett syndrome (RTT), a postnatal neurodevelopmental disorder, is caused by mutations in the methyl-CpG-binding protein 2 (*MECP2*) gene. Children with RTT display cognitive and motor abnormalities as well as autistic features. We studied mice bearing a truncated *Mecp2* allele (*Mecp2*$^{308/Y}$ mice) and found evidence of increased anxiety-like behavior and an abnormal stress response as evidenced by elevated serum corticosterone levels. We found increased corticotropin-releasing hormone (*Crh*) gene expression in the paraventricular nucleus of the hypothalamus, the central amygdala, and the bed nucleus of the stria terminalis. Finally, we discovered that MeCP2 binds the *Crh* promoter, which is enriched for methylated CpG dinucleotides. In contrast, the MeCP2308** protein was not detected at the *Crh* promoter. This study identifies *Crh* as a target of MeCP2 and implicates *Crh* overexpression in the development of specific features of the *Mecp2*$^{308/Y}$ mouse, thereby providing opportunities for clinical investigation and therapeutic intervention in RTT.**

autism | corticotropin-releasing hormone | methyl-CpG-binding protein 2

Rett syndrome (RTT, MIM 312750) is an X-linked dominant neurological disorder that affects ≈1 in 10,000 females (1). The clinical features of RTT include mental retardation, ataxia, hand stereotypes, seizures, and breathing irregularities (1). In addition, behavioral abnormalities, most prominently social behavior deficits and autistic features, are prominent (1, 2). Mutations in the methyl-CpG-binding protein 2 (*MECP2*) gene, which encodes the MeCP2 protein, account for the vast majority of RTT cases (1, 3). MeCP2 binds methylated CpG dinucleotides in close proximity to an A/T-rich motif (4), and it controls chromatin architecture by recruiting proteins that assist in gene silencing, including histone deacetylases (5, 6), histone methyltransferases (7), DNA methyltransferases (8), and CoREST (9). Additionally, MeCP2 regulates RNA splicing via an interaction with the YB-1 protein (10).

Based on its role in transcriptional repression, mutations that disrupt the normal function of MeCP2 are predicted to result in the misexpression of its targets (11). To date, transcriptional profiling of *Mecp2*-null mice has uncovered only three target genes, *Sgk* (12), *Fkbp5* (12), and *Uqcrc1* (13). Additionally, candidate gene approaches have identified *BDNF* (14, 15) and *DLX5* (16) as MeCP2 targets. Notably, the mechanism(s) by which altered expression of these genes contributes to the RTT neurobehavioral phenotype remains elusive.

Previously, we generated the *Mecp2*^{308} mouse, which carries a hypomorphic *Mecp2* allele in which a truncating mutation is placed after amino acid 308 (17). *Mecp2*^{308} male mice are viable up to 1 year of age and replicate many aspects of human RTT, including cognitive and motor impairments, seizures, and social behavior deficits (17–19). Initial behavioral analysis of *Mecp2*$^{308/Y}$ mice on a highly mixed background indicated that they have increased anxiety in the open field assay (17). Moreover, we noticed a tremor in *Mecp2*$^{308/Y}$ mice that becomes more severe with handling, suggesting that they are easily stressed (B.E.M. and H.Y.Z., unpublished observation). These observations are consistent with findings from clinical investigations of the behavior of RTT patients, which indicate that episodes of heightened anxiety occur more frequently in RTT (up to 75% of cases) than in other forms of mental retardation (2, 20). Anxiety is also reported in cases in which *MECP2* mutations cause additional neurobehavioral phenotypes (21, 22). These features of RTT, together with preliminary observations of the behavior of *Mecp2*$^{308/Y}$ mice, led us to propose that anxiety is an important component of the behavioral phenotype of RTT and that MeCP2 regulates key molecule(s) relevant to this behavior. To test this hypothesis, we performed behavioral and physiologic analyses on *Mecp2*$^{308/Y}$ mice and investigated the effect of *Mecp2* mutation on a molecular pathway that contributes to anxiety-related behaviors.

Results

***Mecp2*$^{308/Y}$ Mice Display Enhanced Levels of Anxiety-Like Behavior.** We evaluated the anxiety-like behavior of *Mecp2*$^{308/Y}$ mice by using the open field (23), the elevated plus maze (24), and the light/dark box (25). In the open field, *Mecp2*$^{308/Y}$ mice explored the center of the arena far less than their WT counterparts ($P = 0.005$) (Fig. 1*A*). In the elevated plus maze, *Mecp2*$^{308/Y}$ mice spent less time in the open arms than WT animals ($P = 0.005$) (Fig. 1*B*). However, there was no difference in the number of total arm entries between genotypes ($P = 0.258$) (Fig. 1*C*), suggesting that reduced open arm activity by *Mecp2*$^{308/Y}$ mice was due to increased anxiety, and not hypoactivity or motor impairment. In the light/dark box, *Mecp2*$^{308/Y}$ mice spent significantly less time in the lit side of the apparatus ($P = 0.010$) (Fig. 1*D*) and made fewer transitions than WT animals ($P = 0.010$) (Fig. 1*E*). Overall, the results of these assays indicate that *Mecp2*$^{308/Y}$ mice display increased anxiety-like behavior compared with WT animals.

***Mecp2*$^{308/Y}$ Mice Have an Enhanced Corticosterone Response to Restraint Stress.** Besides anxiety, the mammalian stress response includes the activation of the hypothalamic-pituitary-adrenal

Author contributions: B.E.M. and H.Y.Z. designed research; B.E.M. and S.F.B. performed research; M.B.Y., J.P.C., and C.T. contributed new reagents/analytic tools; B.E.M. and H.Y.Z. analyzed data; and B.E.M. and H.Y.Z. wrote the paper.

The authors declare no conflict of interest.

Freely available online through the PNAS open access option.

Abbreviations: RTT, Rett syndrome; MECP2, methyl-CpG-binding protein 2; HPA, hypothalamic-pituitary-adrenal; CRH, corticotropin-releasing hormone; ISH, *in situ* hybridization; PVN, paraventricular nucleus of the hypothalamus; CeA, central amygdala; BNST, bed nucleus of the stria terminalis; QRTPCR, quantitative real-time RT-PCR; QPCR, quantitative PCR; seqChIP, sequential ChIP.

‡‡To whom correspondence should be addressed. E-mail: hzoghbi@bcm.tmc.edu.

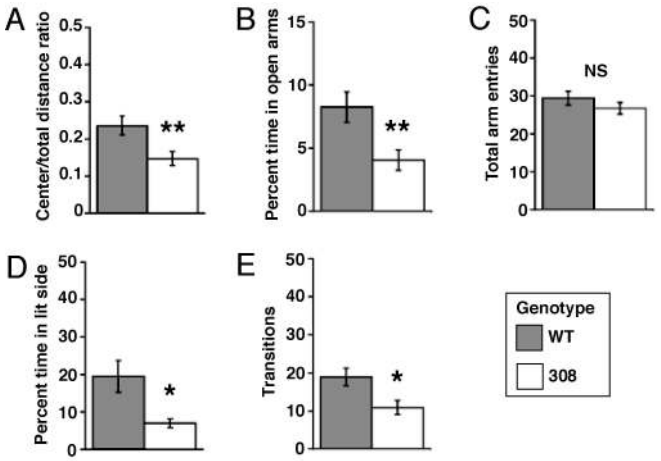

Fig. 1. *Mecp2*$^{308/Y}$ mice display increased levels of anxiety behavior. (*A*) *Mecp2*$^{308/Y}$ mice explored the center of the open field less than WT mice. (*B* and *C*) *Mecp2*$^{308/Y}$ mice spent less time exploring the open arms of the elevated plus maze than WT mice (*B*), but both groups made a similar number of total arm entries (*C*). (*D* and *E*) In the light/dark box, *Mecp2*$^{308/Y}$ spent less time in the lit side of the apparatus (*D*) and made fewer transitions between the two sides of the box than WT mice (*E*). Values represent mean ± SEM. The asterisks indicate significant genotype differences (*, $P < 0.05$; **, $P < 0.01$). NS, nonsignificant effects.

(HPA) axis, which leads to glucocorticoid release from the adrenal cortex into the circulation (26). To determine whether *Mecp2*$^{308/Y}$ mice have a hyperactive HPA axis, we analyzed serum levels of the predominant murine glucocorticoid, corticosterone, in these animals under basal conditions and after 5, 15, and 30 min of acute restraint, as well as 30 min after 30 min of restraint. Both morning and evening basal levels were similar between genotypes ($P = 0.884$ and $P = 0.995$, respectively) (Fig. 2*A*). However, we found a significant effect of treatment ($F_{4,50} = 29.5$, $P = 1.29e{-}12$) and a significant genotype × treatment interaction effect on corticosterone levels after restraint ($F_{4,50} = 3.03$, $P = 0.026$). Specifically, *Mecp2*$^{308/Y}$ mice experienced elevated peak corticosterone levels (786 ± 68 ng/ml) >1.5 times ($P = 0.010$) as high as those measured in WT animals (478 ± 85 ng/ml) (Fig. 2*B*). These results indicate that *Mecp2*$^{308/Y}$ mice have an enhanced physiologic response to stress, characterized by increased HPA axis activity, in addition to an abnormal behavioral response to stress.

***Mecp2*$^{308/Y}$ Mice Overexpress the Corticotropin-Releasing Hormone (*Crh*) Transcript.** Corticotropin-releasing hormone (CRH), a neuropeptide encoded by the *Crh* gene, coordinates the behavioral

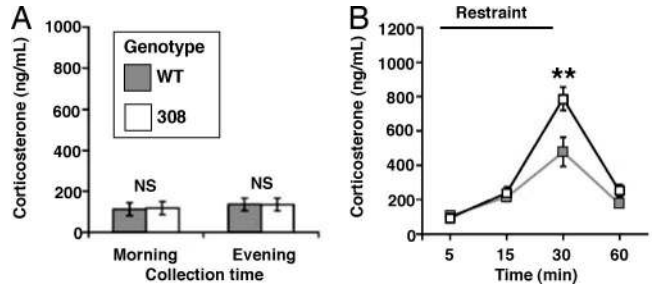

Fig. 2. *Mecp2*$^{308/Y}$ mice have an enhanced corticosterone response to stress. (*A*) Basal morning and evening corticosterone levels are similar between *Mecp2*$^{308/Y}$ and WT mice. (*B*) *Mecp2*$^{308/Y}$ mice (black line) have an enhanced corticosterone response to stress compared with WT mice (gray line), which is evident after 30 min of restraint. Values represent mean ± SEM. The asterisk indicates a significant post hoc *t* test at the 30-min time point (**, $P < 0.01$). NS, nonsignificant effects.

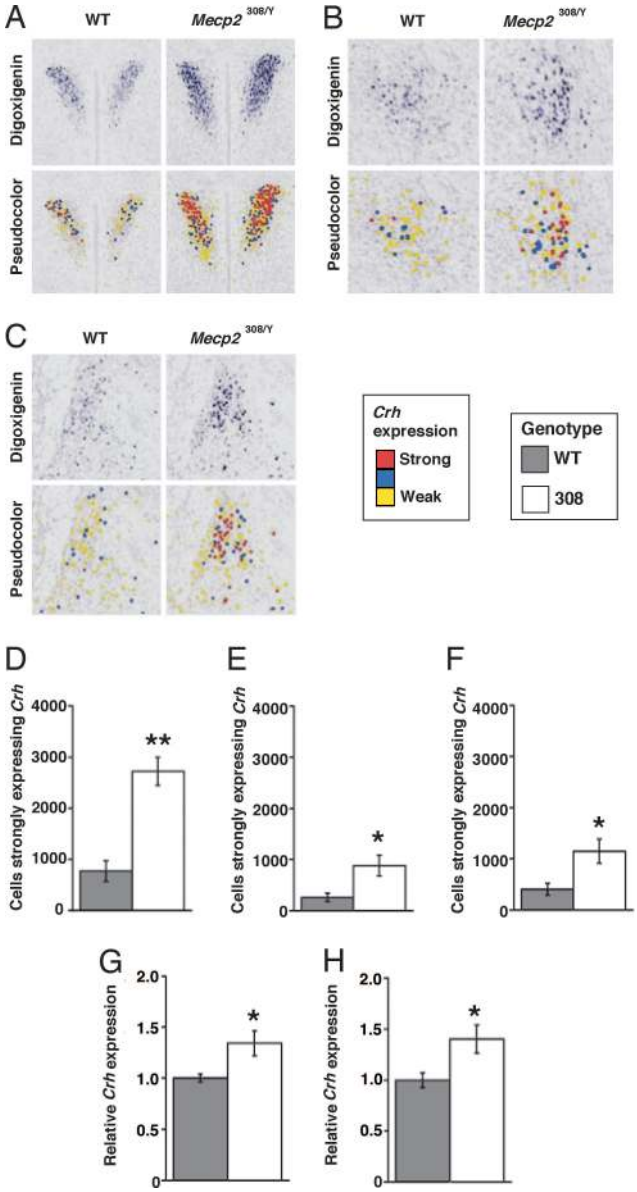

Fig. 3. *Mecp2*$^{308/Y}$ mice have enhanced *Crh* expression in brain regions linked to corticosterone release and fear/anxiety behavior. ISH was performed for *Crh*. Here, we show representative sections from the PVN (*A*), the CeA (*B*), and the BNST (*C*), along with pseudocolored versions of each section demonstrating enhanced *Crh* expression in *Mecp2*$^{308/Y}$ mice compared with WT controls. Quantification of strongly expressing cells in the entire PVN, CeA, or BNST identified by ISH provided evidence of increased *Crh* expression in *Mecp2*$^{308/Y}$ mice (*D*, *E*, and *F*, respectively). QRTPCR confirms enhanced *Crh* expression in the PVN (*G*) and the CeA (*H*) of *Mecp2*$^{308/Y}$ mice. Values represent mean ± SEM. The asterisks indicate significant genotype differences (*, $P < 0.05$; **, $P < 0.01$).

and physiologic response to stress (27). The combination of increased anxiety and elevated stress-induced corticosterone release in *Mecp2*$^{308/Y}$ mice led us to hypothesize that these animals might also have enhanced *Crh* expression. To answer this question, we used *in situ* hybridization (ISH) to localize areas of *Crh* transcription and analyze *Crh* expression levels in the brains of *Mecp2*$^{308/Y}$ and WT mice. We focused our attention on three brain regions: the paraventricular nucleus of the hypothalamus (PVN) (Fig. 3*A*), from which CRH release activates the HPA axis (28); the central amygdala (CeA) (Fig. 3*B*), where CRH promotes a behavioral response akin to conditioned fear; and the

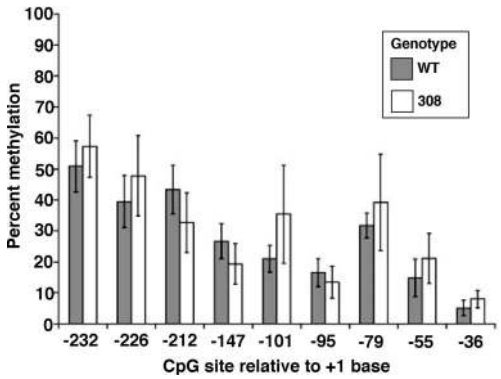

Fig. 4. The *Crh* promoter contains methyl-CpG dinucleotides. Bisulfite sequencing was used to analyze the methylation status of nine CpG sites in the *Crh* promoter of *Mecp2*$^{308/Y}$ and WT mice. Several methylated CpG sites were identified, but there was no effect of genotype on their methylation status. Values represent mean ± SEM.

bed nucleus of the stria terminalis (BNST) (Fig. 3*C*), where CRH elicits anxiety-like behavior (29). We used custom-designed imaging software (30) to count *Crh*-expressing cells from tissue sections that spanned the entirety of these regions in multiple animals. Using this method, we identified a significant effect of genotype on the number of cells strongly expressing *Crh* in the PVN ($P = 1.84e{-}4$) (Fig. 3*D*), the CeA ($P = 0.017$) (Fig. 3*E*), and the BNST ($P = 0.018$) (Fig. 3*F*). We confirmed these results by performing quantitative real-time RT-PCR (QRTPCR) for *Crh* on cDNA derived from the PVN and the CeA of another group of *Mecp2*$^{308/Y}$ and WT mice. Again, we found a significant effect of genotype on *Crh* expression in the PVN ($P = 0.020$) (Fig. 3*G*) and the CeA ($P = 0.022$) (Fig. 3*H*). Collectively, these studies indicate that *Mecp2*$^{308/Y}$ mice overexpress *Crh* in brain regions critical for the behavioral and physiologic responses to stress. Importantly, we assayed expression levels of glucocorticoid receptor and mineralocorticoid receptor RNA, as well as pharmacologic suppression of corticosterone release in *Mecp2*$^{308/Y}$ mice, to evaluate the negative feedback arm of the HPA axis and found that it functions normally (Fig. 7, which is published as supporting information on the PNAS web site). These data suggest that *Crh* overexpression is the primary source of HPA axis dysfuntion in these animals.

MeCP2 Binds to a Conserved, Methylated Region of the *Crh* Promoter. Our finding of *Crh* overexpression in *Mecp2*$^{308/Y}$ mice raised the possibility that MeCP2 might play a role in regulating the transcription of *Crh*. To investigate this possibility, we used bisulfite sequencing (31) to determine whether hypothalamic DNA contains methylated CpG sites at the *Crh* promoter and whether such methylation differs between *Mecp2*$^{308/Y}$ and WT mice. We examined the 337 bp closest to the start site; among these 337 bp were nine CpG sites that are conserved between mice and humans (Fig. 8, which is published as supporting information on the PNAS web site). We found a significant effect of CpG site on methylation frequency ($F_{8,72} = 6.15$, $P = 4.88e{-}6$), indicating that, indeed, some CpG sites were more frequently methylated than others. However, we did not detect an effect of genotype ($F_{1,72} = 0.465$, $P = 0.498$) or a genotype × CpG site interaction effect ($F_{8,72} = 0.448$, $P = 0.888$) on methylation frequency (Fig. 4). This finding assured us that the increase in *Crh* expression is not secondary to methylation differences at the promoter.

Next, to determine whether MeCP2 binds the *Crh* promoter, we performed ChIP on brain tissue from WT, *Mecp2*$^{308/Y}$, and *Mecp2*-null mice with an antibody specific to the N terminus of MeCP2, a region of MeCP2 that is present in both the WT MeCP2 and the MeCP2^{308} truncated protein. The DNA fragments recovered were used as template for quantitative PCR (QPCR) employing primer sets that spanned the region from 3.5 kb upstream to 1.7 kb downstream of the +1 site of *Crh*, an area that includes the conserved promoter, the sole intron, and nearly the entire coding sequence of the gene (Fig. 5*A*). Compared with ChIP on *Mecp2*-null chromatin, ChIP on WT chromatin with this antibody enriched for the methylated domain of the *Crh* promoter, but ChIP on *Mecp2*$^{308/Y}$ chromatin did not enrich for any region of *Crh* analyzed (Fig. 5 *B* and *D*). Statistical analysis of the QPCR data using a two-way ANOVA revealed a significant effect of genotype ($F_{1,36} = 223.9$, $P = 4.99e{-}17$) and region ($F_{5,36} = 2.56$, $P = 0.045$), as well as a significant genotype × region interaction ($F_{5,36} = 2.87$, $P = 0.028$). Similar results were obtained when we performed ChIP with an antibody specific to the C terminus of MeCP2, a region of MeCP2 that is present in WT MeCP2, but not MeCP2^{308} protein (Fig. 5 *C* and *D*). Again, a two-way ANOVA revealed a significant effect of genotype ($F_{1,36} = 150.1$, $P = 2.1e{-}14$) and region ($F_{5,36} = 2.89$, $P = 0.027$), as well as a significant genotype × region interaction ($F_{5,36} = 2.97$, $P = 0.024$). Collectively, these results point to a specific association between WT MeCP2 and the methylated promoter region of *Crh in vivo*. In contrast, the MeCP2^{308} protein was not detected at the *Crh* promoter.

MeCP2 suppresses transcription by recruiting corepressors to DNA (5–9). Given our observation that MeCP2 binds the *Crh* promoter, we sought to confirm the repressive function of MeCP2 at this locus. To this end, we performed sequential ChIP (seqChIP) on WT mouse brain tissue. The first round (primary) ChIP was conducted with antibodies against acetylated histone H3, a mark of transcriptionally active chromatin, or dimethyl-histone H3 Lys-9, a mark of transcriptionally inactive chromatin (32). We used anti-C-terminal MeCP2 for the second round (secondary) ChIP, which we performed on half of the product of the primary ChIP; the remaining sample was saved for analysis of the primary ChIP. DNA recovered from both ChIP steps was analyzed by QPCR for the presence of the *Crh* promoter. In this way, we were able to simultaneously evaluate the activity state of *Crh* as well as MeCP2 binding to the *Crh* promoter.

When we performed the primary ChIP, we recovered more *Crh* promoter with anti-acetyl histone H3 than when we used anti-dimethyl histone H3 Lys-9 (Fig. 6*A*, $P = 0.006$), suggesting that the majority of cells express some baseline level of *Crh*. However, when we performed the second round ChIP with anti-MeCP2, we recovered significantly more *Crh* from chromatin that had been initially immunoprecipitated with anti-dimethyl-histone H3 Lys-9 than from chromatin that had been initially immunoprecipitated with anti-acetyl histone H3 (Fig. 6*B*, $P = 0.029$). Thus, the results of seqChIP indicate that MeCP2 preferentially associates with a transcriptionally inactive, dimethyl-histone H3 Lys-9-rich form of the *Crh* promoter in mice.

Discussion

In this study, we identify *Crh* as a target of MeCP2 and we describe behavioral and physiologic phenotypes in *Mecp2*$^{308/Y}$ mice that are consistent with enhanced CRH signaling. Behaviorally, CRH induces anxiety (27). For example, intracerebroventricular delivery of CRH into the central nervous system of rodents is anxiogenic (27). Likewise, transgenic mice overexpressing *Crh* have enhanced anxiety (27). Conversely, pharmacologic antagonists of CRH receptor-1 signaling are anxiolytic, and *Crhr1* knockout mice have reduced anxiety (27). CRH signaling in the CeA and the BNST are particularly critical to producing these behavioral effects (29). Given the established role of CRH in anxiety, it is likely that the anxiety phenotype that

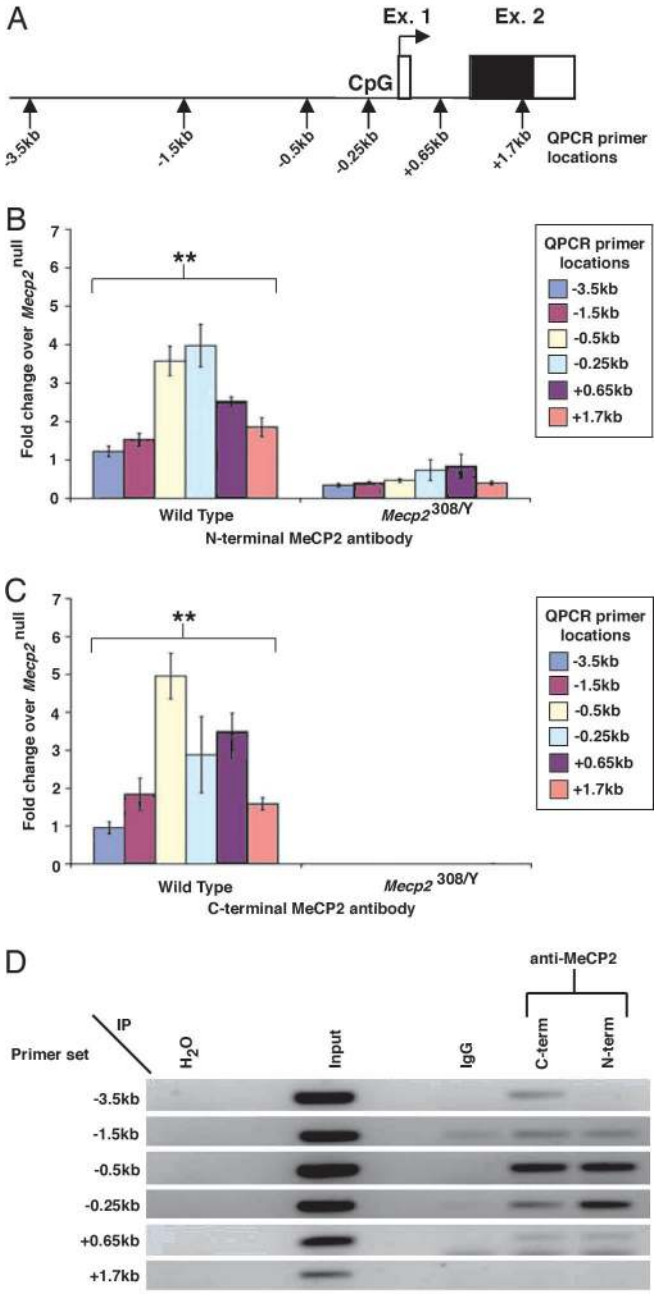

Fig. 5. The *Crh* promoter is bound by MeCP2, but not MeCP2^{308}, *in vivo*. (*A*) *Crh* consists of two exons (Ex. 1 and Ex. 2) flanking a single intron. The second exon contains the coding region of *Crh* (shaded part of Ex. 2). A putative CpG island (CpG) lies in the promoter. Approximate regions of chromatin-immunoprecipitated DNA amplified by QPCR are identified by arrows. ChIP was performed on whole brain lysate from *Mecp2*$^{308/Y}$ and WT mice by using antibody specific to the N terminus (*B*) or the C terminus (*C*) of MeCP2, and QPCR was used to quantify *Crh* DNA in each immunoprecipitate. (*D*) We also performed nonquantitative PCR on these samples. The PCR products were run on agarose gels and visualized by ethidium bromide staining. Shown here are results representative of PCR using primers that covered the same regions of *Crh* as the QPCR primers. (*B* and *C*) Asterisks indicate an overall effect of genotype on the amount of DNA recovered by ChIP (**, $P < 0.01$). Values represent mean ± SEM.

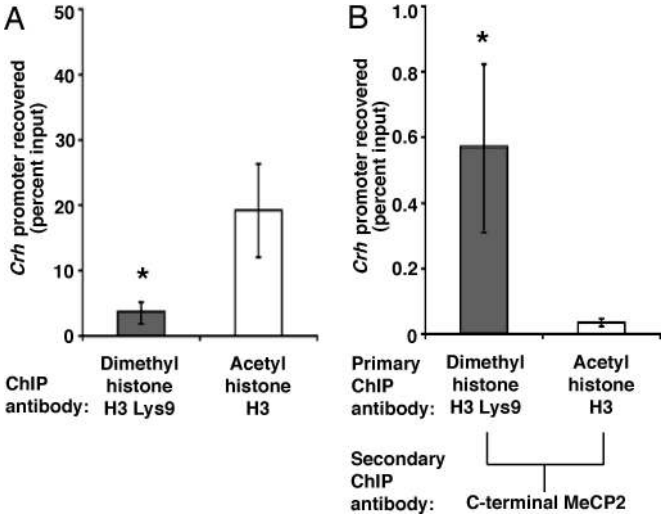

Fig. 6. Under basal conditions *in vivo*, MeCP2 is bound to a repressed form of the *Crh* promoter. SeqChIP was performed on hypothalamic chromatin from WT mice. (*A*) More *Crh* was recovered when the primary ChIP was conducted with anti-acetyl histone H3 than when it was conducted with anti-dimethyl-histone H3 Lys-9. (B) Secondary ChIP with anti-C-terminal MeCP2 on the samples recovered in *A* indicates that MeCP2 preferentially associates with dimethyl-histone H3 Lys-9 at the *Crh* promoter. Values represent mean ± SEM. The asterisks are used to indicate significant differences (*, $P < 0.05$).

we observed in *Mecp2*$^{308/Y}$ mice is linked to enhanced *Crh* expression in the BNST and the CeA.

Like the behavioral effects of CRH, the effects of CRH on the physiologic response to stress are well known. CRH produced in the PVN initiates HPA axis activation and elicits glucocorticoid release from the adrenal cortex (28). Thus, exogenous administration of CRH in the PVN of rodents transiently increases circulating corticosterone, and transgenic overexpression of *Crh* chronically elevates serum glucocorticoid levels (27). Conversely, CRH antagonists block glucocorticoid release, and both CRH and CRH receptor-1 knockout mice have blunted post-stress serum glucocorticoid concentrations (27). We found evidence of elevated stress-induced serum corticosterone levels and increased *Crh* expression in the PVN of *Mecp2*$^{308/Y}$ mice compared with controls. Given the role of PVN CRH in stimulating the HPA axis (28), it is likely that enhanced *Crh* expression in the PVN of *Mecp2*$^{308/Y}$ mice is behind the hypercorticosteronemia phenotype that we identified. Thus, enhanced *Crh* expression in *Mecp2*$^{308/Y}$ mice seems to explain both the physiologic and the behavioral phenotypes of these animals that we describe here.

Interestingly, increased anxiety-like behavior and HPA axis hyperactivity are not limited to *Mecp2*$^{308/Y}$ mice but seem to be features that are shared by other mouse models of RTT as well as humans with RTT. Gemelli *et al*. observed increased anxiety-like behavior in conditional *Mecp2* knockout mice (33), whereas constitutive *Mecp2*-null mice demonstrate a trend toward increased serum glucocorticoid levels and have enhanced expression of two glucocorticoid-inducible genes, *Sgk* and *Fkbp5* (12). We analyzed *Crh* expression in *Mecp2*-null mice, but we did not detect any significant abnormalities, possibly because of the time at which we tested them or other features of this mutant (data not shown). With regard to humans with RTT, careful surveys indicate that anxiety-like behaviors occur frequently (2, 20). Furthermore, there is evidence of increased urinary cortisol excretion in girls with RTT (34), suggesting that humans with *MECP2* mutations also experience elevated serum glucocorticoid levels. Given these data, the results of our analysis of *Mecp2*$^{308/Y}$ mice support the conclusion that anxiety and HPA axis hyperactivity are components of the phenotype produced by *MECP2* mutations.

The behavioral and physiologic data show that *Mecp2*$^{308/Y}$ mice are exposed to high levels of CRH and corticosterone. Interestingly, some of the chronic effects of these compounds resemble characteristic aspects of RTT. Specifically, decreased dendritic branching, reduced synaptic plasticity, and memory impairment are features observed in the context of repeated glucocorticoid exposure (35), exposure to high concentrations of CRH (36, 37), and *Mecp2*/*MECP2* mutation (19, 38–40). These similarities suggest that an overabundance of CRH and/or glucocorticoids might contribute to other aspects of the RTT phenotype beyond anxiety-like behaviors. In the future, clinical studies should examine the HPA axis in children with RTT and determine whether misregulation of *CRH* and/or glucocorticoids contributes to additional phenotypes associated with *MECP2* mutations.

MeCP2 modulates the transcriptional activity of *Crh* in WT mice, but *Crh* transcriptional regulation is impaired in *Mecp2*$^{308/Y}$ mice. Our results indicate that CpG methylation at the *Crh* promoter is unaltered in the *Mecp2*$^{308/Y}$ mice, suggesting that enhanced *Crh* expression in *Mecp2*$^{308/Y}$ mice is due to a functional defect in the MeCP2^{308} protein itself. Whereas the exact biochemical mechanism that prevents the MeCP2^{308} protein from properly regulating *Crh* transcription remains unidentified, the simplest explanation is either that the MeCP2^{308} protein is unable to bind the *Crh* promoter or that it binds with reduced affinity. However, we cannot exclude the possibility that the MeCP2^{308} protein is not pulled down under our assay conditions.

It has been hypothesized that RTT phenotypes are due to the misexpression of MeCP2 target genes (11). Here, we show that WT MeCP2 binds to the *Crh* promoter. We also describe enhanced *Crh* expression in *Mecp2*$^{308/Y}$ mice together with behavioral and physiologic phenotypes consistent with heightened levels of CRH. Additionally, we do not detect the MeCP2^{308} protein at the *Crh* promoter. This observation provides both a plausible explanation for enhanced *Crh* expression in *Mecp2*$^{308/Y}$ mice and a viable connection between MeCP2 dysfunction and the behavioral and physiologic phenotypes of these animals. Based on our findings, we propose that impaired regulation of *CRH* expression contributes to the anxiety behavior and increased cortisol levels observed in patients with RTT. Thus, in this study, we identify *Crh* as an MeCP2 target gene to which specific, quantifiable components of the RTT phenotype can be attributed. Importantly, our understanding of the basic biology of *Crh* regulation in a mouse model of RTT will allow us to evaluate pathway-specific pharmacologic and genetic interventions aimed at relieving the behavioral and physiologic abnormalities that we describe here. Such studies will provide a first step toward mechanism-based translational studies in RTT.

Materials and Methods

Animals. We used littermate pairs of WT and *Mecp2*$^{308/Y}$ animals that were the F_1 offspring of 129SvEv females heterozygous for the *Mecp2*^{308} allele crossed with WT C57BL/6J males. *Mecp2*$^{308/Y}$ males were used to avoid the confounding effects of X chromosome inactivation (41).

Behavioral Studies. Behavioral tests were performed on 4-month-old male mice during the light period (0900–1300; lights on 0700–1900). We maintained lighting at 50 lux and used a white-noise generator (Lafayette Instruments, Lafayette, IN) to maintain ambient background noise at 60 dB. For the open field assay, mice (n = 29 per genotype) were placed in the center of a 40 × 40 × 30-cm arena, and their activity was quantified over a 30-min period by a computer-operated Digiscan optical animal activity system (Acuscan, Columbus, OH). The elevated plus maze consists of two opposing closed arms (25 × 7.5 × 15.5 cm) and two opposing open arms (25 × 7.5 × 0.5 cm) connected to a center platform (7.5 × 7.5 cm) and elevated 50 cm above the floor. Mice (n = 28 per genotype) were placed in the center of the maze, and their activity was observed for 10 min. The light/dark box consists of a clear plastic chamber (36 × 20 × 26 cm) separated from a covered black plastic chamber (15.5 × 20 × 26 cm) by a black plastic divider with a 10.5 × 5-cm opening. Mice (n = 23 per genotype) were placed at the far end of the lit side, and their activity was observed for 10 min.

Corticosterone Studies and Stress-Induction Protocol. Morning and evening basal corticosterone levels (collected between 0700 and 0900 and between 1700 and 1900, respectively) were obtained from animals (n = 5–9 per genotype) that were undisturbed for 12 h. Stress-induced corticosterone levels were obtained from animals (n = 5–10 per genotype) that were restrained in 50-ml conical tubes. Mice were killed by rapid decapitation, and trunk blood was collected in prechilled tubes containing EDTA. The blood was centrifuged at 0.8 × g for 10 min, and serum was collected and frozen at −80°C until it was analyzed. Serum corticosterone levels were measured by using an enzyme-linked immunoassay (IDS Inc., Fountain Hills, AZ).

***Crh* Expression Analysis.** We generated an ISH probe for *Crh* by using reverse-transcribed mouse cDNA as a template. Primer sequences are published in *Supporting Text*, which is published as supporting information on the PNAS web site. ISH was performed on brain sections from *Mecp2*$^{308/Y}$ and WT mice (n = 6 per genotype) by using a robotic platform as described (42). We performed quantitative analysis of the ISH signal on sections spanning the entire PVN, CeA, and BNST by using the Celldetekt protocol to determine cellular gene expression strengths (30). QRTPCR on cDNA generated from *Mecp2*$^{308/Y}$ and WT mouse brain regions of interest (n = 8–12 per genotype) was performed with TaqMan primers on an ABI 7300 Real Time PCR System (Applied Biosystems, Foster City, CA). Primer sequences for *Crh* and glyceraldehyde-3-phosphate dehydrogenase (*Gapd*), our internal control, are provided in *Supporting Text*.

Sodium Bisulfite Sequencing. We performed sodium bisulfite sequencing on hypothalamic DNA isolated from five WT and *Mecp2*$^{308/Y}$ mice as described (31). Primers and PCR conditions can be found in *Supporting Text*. The PCR product was cloned into the pCR4-TOPO vector (Invitrogen, Carlsbad, CA) and transformed. We prepared 30 minipreps per sample and sequenced 17–27 of these per sample.

ChIP. Our procedure for chromatin isolation and immunoprecipitation, along with TaqMan primer sets used for QPCR,can be found in *Supporting Text*. We analyzed ChIP and seqChIP QPCR data by normalizing to the appropriate input sample and subtracting out background (defined as the normalized quantity recovered by ChIP with nonspecific IgG). For data in Fig. 5, we calculated the fold enrichment over the normalized quantity recovered by ChIP on *Mecp2*-null chromatin. Means were calculated from four independent ChIPs with each antibody on WT and *Mecp2*$^{308/Y}$ chromatin, as well as from six independent seqChIP experiments.

Statistics. Two-way ANOVA was used to analyze the time course of corticosterone release after restraint (genotype × time interval); the results of bisulfite sequencing (genotype × CpG site); and the results of QPCR mapping of the MeCP2-binding site in the *Crh* promoter (genotype × primer site). We used post hoc t tests with Bonferroni correction to compare genotype differences in corticosterone release at discrete time points after restraint. We used Student's t test to analyze measures recorded in the open field assay, elevated plus maze, and the light/dark box; basal corticosterone levels; gene expression ratios obtained

by QRTPCR; and the number of cells strongly expressing *Crh* by ISH. A nonparametric Mann–Whitney test was used to analyze the results of the seqChIP experiment. We consistently used two-sided tests and $\alpha = 0.05$ to determine statistical significance. Results are presented as mean ± SEM.

We thank Gregor Eichele for his advice regarding *in situ* hybridization, Marwan Shinawi for controls and protocols for bisulfite sequencing, Juan Young for advice on the restraint stress protocol, E. O'Brian Smith and Mariella DeBiasi for helpful discussions, and the Zoghbi laboratory members for their critical input. This work was supported by National Institutes of Health (NIH) Fellowship F30 MH068996 (to B.E.M.); National Library of Medicine Grant 5T15LM07093 from the Keck Center for Computational and Structural Biology, and National Center for Research Resources Grant P41 RR02250 (to J.P.C.); NIH Grant R01 HD40301 (to H.Y.Z.); and Core Laboratories of the Mental Retardation and Developmental Disabilities Research Center Grant P30 HD024064. H.Y.Z. is an investigator with the Howard Hughes Medical Institute.

1. Moretti P, Zoghbi HY (2006) *Curr Opin Genet Dev* 16:276–281.
2. Mount RH, Charman T, Hastings RP, Reilly S, Cass H (2002) *J Child Psychol Psychiatry* 43:1099–1110.
3. Amir RE, Van den Veyver IB, Wan M, Tran CQ, Francke U, Zoghbi HY (1999) *Nat Genet* 23:185–188.
4. Klose RJ, Sarraf SA, Schmiedeberg L, McDermott SM, Stancheva I, Bird AP (2005) *Mol Cell* 19:667–678.
5. Jones PL, Veenstra GJ, Wade PA, Vermaak D, Kass SU, Landsberger N, Strouboulis J, Wolffe AP (1998) *Nat Genet* 19:187–191.
6. Nan X, Ng HH, Johnson CA, Laherty CD, Turner BM, Eisenman RN, Bird A (1998) *Nature* 393:386–389.
7. Fuks F, Hurd PJ, Wolf D, Nan X, Bird AP, Kouzarides T (2003) *J Biol Chem* 278:4035–4040.
8. Kimura H, Shiota K (2003) *J Biol Chem* 278:4806–4812.
9. Lunyak VV, Burgess R, Prefontaine GG, Nelson C, Sze SH, Chenoweth J, Schwartz P, Pevzner PA, Glass C, Mandel G, Rosenfeld MG (2002) *Science* 298:1747–1752.
10. Young JI, Hong EP, Castle JC, Crespo-Barreto J, Bowman AB, Rose MF, Kang D, Richman R, Johnson JM, Berget S, Zoghbi HY (2005) *Proc Natl Acad Sci USA* 102:17551–17558.
11. Caballero IM, Hendrich B (2005) *Hum Mol Genet* 14(Spec No 1):R19–R26.
12. Nuber UA, Kriaucionis S, Roloff TC, Guy J, Selfridge J, Steinhoff C, Schulz R, Lipkowitz B, Ropers HH, Holmes MC, Bird A (2005) *Hum Mol Genet* 14:2247–2256.
13. Kriaucionis S, Paterson A, Curtis J, Guy J, Macleod N, Bird A (2006) *Mol Cell Biol* 26:5033–5042.
14. Chen WG, Chang Q, Lin Y, Meissner A, West AE, Griffith EC, Jaenisch R, Greenberg ME (2003) *Science* 302:885–893.
15. Martinowich K, Hattori D, Wu H, Fouse S, He F, Hu Y, Fan G, Sun YE (2003) *Science* 302:890–893.
16. Horike S, Cai S, Miyano M, Cheng JF, Kohwi-Shigematsu T (2005) *Nat Genet* 37:31–40.
17. Shahbazian M, Young J, Yuva-Paylor L, Spencer C, Antalffy B, Noebels J, Armstrong D, Paylor R, Zoghbi H (2002) *Neuron* 35:243–254.
18. Moretti P, Bouwknecht JA, Teague R, Paylor R, Zoghbi HY (2005) *Hum Mol Genet* 14:205–220.
19. Moretti P, Levenson JM, Battaglia F, Atkinson R, Teague R, Antalffy B, Armstrong D, Arancio O, Sweatt JD, Zoghbi HY (2006) *J Neurosci* 26:319–327.
20. Sansom D, Krishnan VH, Corbett J, Kerr A (1993) *Dev Med Child Neurol* 35:340–345.
21. Cohen D, Lazar G, Couvert P, Desportes V, Lippe D, Mazet P, Heron D (2002) *Am J Psychiatry* 159:148–149.
22. Couvert P, Bienvenu T, Aquaviva C, Poirier K, Moraine C, Gendrot C, Verloes A, Andres C, Le Fevre AC, Souville I, *et al*. (2001) *Hum Mol Genet* 10:941–946.
23. Paylor R, Nguyen M, Crawley JN, Patrick J, Beaudet A, Orr-Urtreger A (1998) *Learn Mem* 5:302–316.
24. Pellow S, File SE (1986) *Pharmacol Biochem Behav* 24:525–529.
25. Crawley J, Goodwin FK (1980) *Pharmacol Biochem Behav* 13:167–170.
26. Koob GF (1999) *Biol Psychiatry* 46:1167–1180.
27. Bale TL, Vale WW (2004) *Annu Rev Pharmacol Toxicol* 44:525–557.
28. Bruhn TO, Plotsky PM, Vale WW (1984) *Endocrinology* 114:57–62.
29. Walker DL, Toufexis DJ, Davis M (2003) *Eur J Pharmacol* 463:199–216.
30. Carson JP, Eichele G, Chiu W (2005) *J Microsc (Oxford)* 217:275–281.
31. Frommer M, McDonald LE, Millar DS, Collis CM, Watt F, Grigg GW, Molloy PL, Paul CL (1992) *Proc Natl Acad Sci USA* 89:1827–1831.
32. Fischle W, Wang Y, Allis CD (2003) *Curr Opin Cell Biol* 15:172–183.
33. Gemelli T, Berton O, Nelson ED, Perrotti LI, Jaenisch R, Monteggia LM (2006) *Biol Psychiatry* 59:468–476.
34. Motil KJ, Schultz RJ, Abrams S, Ellis KJ, Glaze DG (2006) *J Pediatr Gastroenterol Nutr* 42:419–426.
35. McEwen BS (1999) *Annu Rev Neurosci* 22:105–122.
36. Brunson KL, Eghbal-Ahmadi M, Bender R, Chen Y, Baram TZ (2001) *Proc Natl Acad Sci USA* 98:8856–8861.
37. Chen Y, Bender RA, Brunson KL, Pomper JK, Grigoriadis DE, Wurst W, Baram TZ (2004) *Proc Natl Acad Sci USA* 101:15782–15787.
38. Armstrong DD (2005) *J Child Neurol* 20:747–753.
39. Hagberg B, Aicardi J, Dias K, Ramos O (1983) *Ann Neurol* 14:471–479.
40. Nelson ED, Kavalali ET, Monteggia LM (2006) *Curr Biol* 16:710–716.
41. Young JI, Zoghbi HY (2004) *Am J Hum Genet* 74:511–520.
42. Yaylaoglu MB, Titmus A, Visel A, Alvarez-Bolado G, Thaller C, Eichele G (2005) *Dev Dyn* 234:371–386.